Epileptic seizure prediction from eigen-wavelet multivariate selfsimilarity analysis of multi-channel EEG signals

Charles-Gérard Lucas, Patrice Abry
ENSL, CNRS, Laboratoire de physique, F-69342 Lyon, France.
firstname.lastname@ens-lyon.fr

Herwig Wendt
IRIT, Univ. Toulouse, CNRS, Toulouse, France.
herwig.wendt@irit.fr

Gustavo Didier
Math. Dept., Tulane University, New Orleans, USA
gdidier@tulane.edu

***Abstract*—Epileptic patients may suffer from severe brain damages during seizures. There is thus a significant need for automated seizure prediction. Independently, brain macroscopic activity has been shown to display scalefree temporal dynamics, which, in turn, were involved into seizure prediction. Selfsimilarity, the paradigm model for scalefree dynamics, has however mostly been defined in univariate settings, thus yielding a collection of independent analyses of recorded signals. Yet, non-negligible correlations exist in multi-channel recordings of brain activity and may prove useful in seizure prediction. This work aims to assess the benefits of using a recently developed multivariate eigen-wavelet framework for multivariate selfsimilarity analysis in seizure prediction using CHB-MIT Scalp EEG data.**

***Index Terms*—Multivariate selfsimilarity, multivariate wavelet transform, EEG data, Epilepsy, seizure prediction.**

I. Introduction

Context. Epilepsy, a chronic disease is a central nervous system disorder, that leads to seizures during which the brain of patients can be severely injured. Devising automated epileptic seizure prediction procedures thus constitutes a crucial stake, notably when they can be implemented from non-invasive and wearable scalp electroencephalogram (EEG) devices.

Numerous studies have shown that infraslow brain activity can be well-described by means of arrhythmic, or scalefree, temporal dynamics and thus efficiently modeled by selfsimilarity [1]–[3]. In practice, selfsimilarity analysis consists in the estimation of a selfsimilarity exponent [4]. Yet, selfsimilarity has been mostly studied in univariate settings, i.e., selfsimilarity exponents are estimated independently for each time series. However, jointly recorded brain activity is monitored via numerous sensors, entailing multivariate time series. Recently, a multivariate selfsimilarity model, operator fractional Brownian motion (ofBm) was proposed [5], and a corresponding multivariate eigen-wavelet-based analysis was developed [4], [6]. The goal of the present work is to study the relevance of using multivariate selfsimilarity for the prediction of epileptic seizures.

Supported by PhD Grant DGA/AID (no 01D20019023), ANR-16-CE33-0020 MultiFracs, ANR-18-CE45-0007 MUTATION. G. Didier's long term visits to ENS Lyon were sponsored by ENS Lyon, the CNRS and the Simons Foundation collaboration grant #714014.

Related works. Seizure prediction is an important research topic, often investigated using tools such as synchronization and functional connectivity [7], phase coherence [8], power spectral density [9], [10], cross-power spectral density [11] or power of the wavelet coefficients [12] in standard frequency bands, autoregressive models, or more recently deep learning frameworks [13]–[15]. Moreover, feature extraction for seizure prediction often involves channel selection to decrease computational complexity or reduce overfitting (see [16] for a review). Scalefree dynamics has also been used in seizure prediction (e.g., from intracranial EEG [17] or single scalp EEG [18]). Fractional Brownian motion (fBm) has been shown to be a relevant model for scalefree temporal dynamics and often used in magnetoencephalogram (MEG) [3] and EEG [2] data analysis. Nevertheless, most works rely on univariate selfsimilarity (or multifractal) analysis. Multivariate selfsimilarity analysis models such as ofBm [4], [6], [19] provide a framework for more efficiently accounting for cross-temporal scalefree dynamics in EEG time series. So far, this has never been studied.

Goals, contributions and outline. This work aims to quantify the relevance and benefits of using multivariate selfsimilarity models and eigen-wavelet-based analysis for epileptic seizure prediction, compared to univariate analysis, using multi-channel scalp EEG recordings. To that end, Section II reviews the ofBm model and the associated wavelet eigenvalue-based multivariate analysis entailing the estimation of M selfsimilarity exponents, compared against classical pairwise multivariate analysis involving the estimation of $M(M-1)/2$ selfsimilarity exponents. This is applied to $M = 22$-variate EEG data, from the CHB-MIT Scalp EEG database [20], described in Section III. Section IV quantifies the significance of multivariate selfsimilarity analysis for epileptic seizure prediction: i) Clear differences in scalefree dynamics, quantified by selfsimilarity exponents, are reported between interictal states (far from seizure) and preictal states (immediately prior to seizure) ; ii) Improved seizure prediction performance are reported for the proposed eigenvalue-based multivariate analysis compared to classical multivariate analysis and to M independent univariate analysis.

II. Multivariate selfsimilarity

Operator fractional Brownian motion. Fractional Brownian motion (fBm), the only Gaussian, self-similar stochastic process with stationary increments, is the reference model for univariate selfsimilarity [21], [22]. Multivariate time series conveying brain activity can be modeled as a collection of M possibly correlated fBm $X \triangleq \{X_{H_1}(t), \ldots, X_{H_M}(t)\}_{t\in\mathbb{R}}$ each associated with a possibly different selfsimilarity parameter H_m. Further, these M-fBm are possibly linearly mixed via a $M \times M$ real-valued invertible matrix W, $Y \triangleq WX = W\{X_{H_1}(t), \ldots, X_{H_M}(t)\}_{t\in\mathbb{R}}$. The resulting multivariate process Y is a specific case of *operator fractional Brownian motion* (ofBm) [4], [6]. Multivariate selfsimilarity analysis thus amounts to estimating, from the observation of Y, the vector of selfsimilarity parameters $\underline{H} = (H_1, \ldots, H_M)$.

Multivariate wavelet analysis. Selfsimilarity is classically analyzed through a wavelet-based representation. Let $D_{Y_m}(2^j, k) = \langle 2^{-j/2}\psi_0(2^{-j}t - k)|Y_m(t)\rangle$, $\forall k \in \mathbb{Z}$, $\forall j \in \{j_1, \ldots, j_2\}$ denote the discrete wavelet transform (DWT) coefficients of component Y_m, where ψ_0 stands for the reference mother wavelet [23]. Multivariate DWT is defined naturally as the collection of univariate DWT applied to each component Y_m: $D_Y(2^j, k) = (D_{Y_1}(2^j, k), \ldots, D_{Y_M}(2^j, k))$, $\forall k \in \mathbb{Z}$, $\forall j \in \{j_1, \ldots, j_2\}$, $\forall m \in \{1, \ldots, M\}$. The wavelet spectrum is then defined as the collection of covariance matrices of $D_Y(2^j, k)$, computed independently at each scale 2^j:

$$S(2^j) \triangleq \frac{1}{n_j}\sum_{k=1}^{n_j} D_Y(2^j, k)D_Y(2^j, k)^*, \tag{1}$$

with n_j the number of wavelet coefficients at scale 2^j. Selfsimilarity analysis consists in the estimation of the exponents $\underline{H} = (H_1, \ldots, H_M)$ from the M-variate time series Y.

Univariate selfsimilarity analysis. First, M independent univariate analyses can be conducted using only the diagonal entries $S_{m,m}(2^j)$ of the wavelet spectrum. When there is no mixing, ($W \equiv I$), $S_{m,m}(2^j)$ asymptotically behave as power-laws across scales, with scaling exponent $2H_m - 1$, thus leading to linear regression-based estimators of $\underline{H}$ [4], [6]:

$$\hat{H}_m^U = \left(\sum_{j=j_1}^{j_2} v_j \log_2 S_{m,m}(2^j)\right)/2 - \frac{1}{2}, \quad m = 1, \ldots, M, \tag{2}$$

with v_j regression weights chosen such that $\sum_j jv_j = 1$ and $\sum_j v_j = 0$ (cf. [4]). When linear mixing is present ($W \neq I$), $S_{m,m}(2^j)$ behave as a mixture of power laws across scales, thus leading to biased estimations of the selfsimilarity parameters. Furthermore, univariate analysis does not exploit cross-temporal dynamics likely to exist in data.

Classical multivariate selfsimilarity analysis. To account for cross-temporal dependencies amongst components, the off-diagonal entries $S_{m,m'}(2^j)$ ($m' \neq m$) can be used. The entries $S_{m,m'}(2^j)$ asymptotically behave as power-laws across scales, with scaling exponent $2H_{m,m'} - 1$, where, without mixing, $H_{m,m'} = (H_m + H_{m'})/2$. This naturally leads to estimate $H_{m,m'}$ by a linear regression:

$$\hat{H}_{m,m'} = \left(\sum_{j=j_1}^{j_2} v_j \log_2 |S_{m,m'}(2^j)|\right)/2 - \frac{1}{2}, \quad m \leq m'. \tag{3}$$

Without mixing ($W = I$), departures of $\hat{H}_{m,m'}$ from $(H_m + H_{m'})/2$ may quantify departures of data from the ofBm model, a potentially valuable multivariate information. When linear mixing is present, these $M(M-1)/2$ estimates lead to biased estimation of $\underline{H}$ [22].

Eigen-wavelet multivariate selfsimilarity analysis. To account both for cross-dependencies and mixing, an alternative *eigen-wavelet*-based multivariate selsimilarity analysis was proposed [4]. It shows that each of the eigenvalues $\lambda_m(2^j)$ of the wavelet spectrum $S(2^j)$ asymptotically behaves as power law with respect to the scales 2^j, with scaling exponent $2H_m - 1$, both with and without mixing.

This naturally suggests to perform the practical estimation of H_m by a linear regression of $\log_2 \lambda_m(2^j)$ against octaves $j = \log_2 2^j$. However, this results in biased estimated due to eigenvalue repulsions of varying strengths across scales caused by limited and different numbers n_j of coefficients available for the estimation of the wavelet spectrum $S(2^j)$. By nature of multiscale analysis, this bias increases at coarser scales because n_j decreases, essentially as $n/2^j$ [19]. To overcome this issue, it was proposed to compute several wavelet spectra at each scale, from non-overlapping time windows $w = 1, \ldots, 2^{j_2-j}$, using an identical number n_{j_2} of wavelet coefficients common to all scales [19]:

$$S^{(w)}(2^j) \triangleq \frac{1}{n_{j_2}}\sum_{k=1+(w-1)n_{j_2}}^{wn_{j_2}} D_Y(2^j, k)D_Y(2^j, k)^*. \tag{4}$$

The eigenvalues $\{\lambda_1^{(w)}(2^j), \ldots, \lambda_M^{(w)}(2^j)\}$ of $S^{(w)}(2^j)$ are computed for each non-overlapping window w at each scale 2^j, entailing a similar repulsion effect at all scales, thus leading to an unbiased estimation of H_m. In practice, the exponents $H_1, \ldots, H_M$ are thus estimated by means of linear regressions over the octaves j of the log-averaged eigenvalues $\log_2 \bar{\lambda}_m(2^j) \triangleq 2^{j-j_2}\sum_{w=1}^{2^{j_2-j}} \log_2(\lambda_m^{(w)}(2^j))$:

$$\hat{H}_m^M = \left(\sum_{j=j_1}^{j_2} v_j \log_2 \bar{\lambda}_m(2^j)\right)/2 - \frac{1}{2}, \quad m = 1, \ldots, M. \tag{5}$$

For a detailed study of performance, see [19].

III. Epilepsy dataset

Data description. Data used in this work consist of multi-channel scalp EEG recordings from the CHB-MIT Scalp EEG database available at https://physionet.org/content/chbmit/1.0.0/, documented in [20]. These recordings have been collected at the Boston Children's Hospital from pediatric subjects with medically intractable seizures and sampled at 256Hz. EEG recordings have been divided into 23 cases collected from 22

subjects, composed of 5 males and 17 females, annotated with beginnings and ends of epileptic seizures. For each subject, 22 to 26 EEG signals were recorded for several hours according to the International 10-20 system of EEG electrode positions and nomenclature. The recordings are at least one-hour long and only a part of them contains seizures.

Data preprocessing. We make use of the 22 first EEG channels, so as to use the same channels for all subjects.

Because the work focuses on predicting epilepsy, the goal is to detect preictal states, which are periods occurring a few minutes before the onset of an epileptic seizure. Thus windows corresponding to preictal states are selected in recordings containing seizures while windows corresponding to interictal states (far in time from any epilectic seizure) are selected in recordings with no seizure. In practice, 2-minute long windows (corresponding to 30720 samples) are used.

To assess quantitatively the performance of the proposed multivariate eigen-wavelet-based selfsimilarity analysis to detect preictal states, only subjects with at least 110 interictal and 10 preictal windows are considered. Thus, only 8 subjects are studied in this work.

IV. Prediction of Preictal States

A. Analysis set-up

Wavelet transforms are computed from 2-minute long windows of the scalp EEG signals, using Daubechies wavelets with $N_\psi = 2$ vanishing moments. Linear regressions are performed across scales 2^1 to 2^4, corresponding to equivalent frequencies ranging from 10Hz to 85Hz. Indeed, intracranial EEG signals are documented to have scalefree dynamics across this range of frequencies [17]. The relevance of this range of scale to account for scalefree dynamics in scalp EEG data is further assessed below.

B. Single-window multivariate analysis

Fig. 1(left) compares, for a preictal window of a given subject, the $M = 22$ univariate wavelet analysis $\log_2 S_{m,m}(2^j)$ (solid blue lines with '+') against the eigen-wavelet-based multivariate analysis $\log_2 \bar{\lambda}_m(2^j)$ (solid red lines with 'o'). While the univariate functions $\log_2 S_{m,m}(2^j)$ mostly superimpose, the multivariate eigenvalue-based analysis clearly shows that 3 eigen-functions $\log_2 \bar{\lambda}_m(2^j)$ take values significantly smaller than and are thus negligible compared to the 19 others, as highlighted for e.g., scale 2^4 in Fig. 2. This suggests linear dependencies amongst the 22 EEG-recordings. A careful inspection of data reveals that EEG time series result from subtraction between electrode measurements, some being used several times, so that one time series actually consists of the addition of several others. Specifically, one time series resulting from the measurements of a pair of two electrodes A and B consists of the addition of other time series measured from pairs of electrodes forming a path from A to B. This lead us to remove three redundant recordings (T7-P7, P3-01, FP2-F4) prior to performing multivariate analysis, thus leading to a $M = 19$-variate selfsimilarity analysis, as reported in Fig. 1(right).

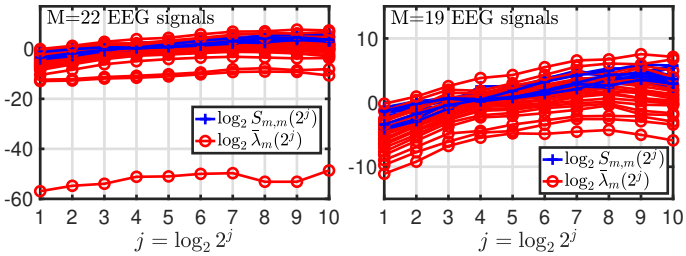

Fig. 1. **Multivariate scalefree analysis.** (blue '+') Diagonal entries $\log_2 S_{m,m}(2^j)$ and (red 'o') log-eigenvalues $\log_2 \bar{\lambda}_m(2^j)$ of the wavelet spectrum $S(2^j)$ for one preictal window associated with Subject 5 before (left) and after (right) removal of 3 redundant channels.

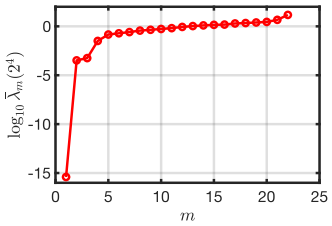

Fig. 2. **Linear dependencies of the 22 EEG signals.** Log-eigenvalues $\log_{10} \bar{\lambda}_m(2^4)$ of the wavelet spectrum $S(2^4)$ for one preictal window associated with Subject 5 and $M = 22$ EEG signals.

Finally, Fig. 1 confirms linear behaviors (hence scalefree dynamics) for both $\log_2 S_{m,m}(2^j)$ and log-eigenvalues $\log_2 \bar{\lambda}_m(2^j)$, $m = 1, \ldots, M$, at fine scales 2^1 to 2^4.

C. Interictal vs. preictal scalefree dynamics

To illustrate the ability of selfsimilarity analysis to detect differences in temporal dynamics of preictal and interictal states, Fig. 3 compares (by means of boxplots) the distributions of the univariate estimates $\hat{H}_m^U$ (left) and eigen-wavelet multivariate estimates $\hat{H}_m^M$ (right) for H_m, for each subject independently. Fig. 3 shows clearer differences between the distributions of estimated preictal and interictal H_m for the eigen-wavelet-based $\hat{H}_m^M$, compared to univariate $\hat{H}_m^U$.

Fig. 3 also shows that detection of interictal vs. preictal states must be conducted on a per-subject basis, as the distributions of reference interictal H_m vary across subjects.

Fig. 3 thus clearly reveals that i) preictal states have temporal dynamics that depart from those of the interictal states for one same subject and ii) interictal states of different subjects have different temporal dynamics. These are the first significant findings of this work.

To quantify differences between preictal and interictal states in distributions of estimated selfsimilarity exponents, Wilcoxon signed-rank test p-values p_m^W are computed. These p-values are compared to Benjamini-Hochberg (multiple hypotheses correction) thresholds, $d_\alpha^{(W,m)}$, at a false discovery rate of $\alpha = 0.05$ [24]. Additionally, an across-component overall performance score is defined as the normalized signed distance from the sorted p-values $p_{\tau(m)}^W$ to Benjamini-Hochberg thresholds $d_\alpha^{(W,m)}$,

$$\text{score} = \frac{1}{M} \sum_{m=1}^{M} (d_\alpha^{(W,m)} - p_{\tau(m)}^W). \qquad (6)$$

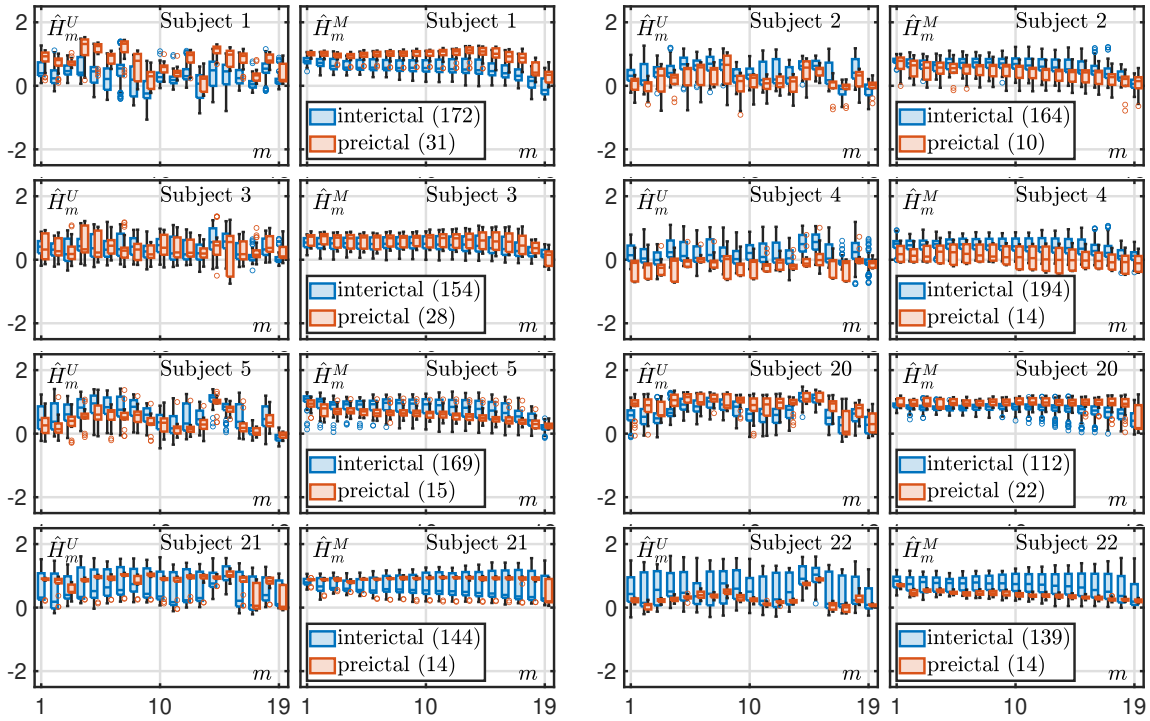

Fig. 3. **Distributions of estimated selfsimilarity parameters.** Boxplots for univariate estimates $\hat{H}_m^U$ (first and third columns) and multivariate estimates $\hat{H}_m^M$ (second and fourth columns) for preictal (red) and interictal (blue) states, for all subjects.

Fig. 4 compares, for each of the 8 subjects, the p-values p_m^W associated with the differences between preictal and interictal states in selfsimilarity exponents. either multivariate $\hat{H}_m^M$ (red 'o') or $\hat{H}_m^U$ (blue '+'), to the Benjamini-Hochberg thresholds $d_\alpha^{(W,m)}$ (black dashed lines) and reports the corresponding scores. Fig. 4 shows that the eigen-wavelet multivariate $\hat{H}_m^M$ lead systematically to lower p-values and thus larger difference scores, and for some subjects significantly so. These findings confirm i) the statistically significant differences between the temporal dynamics of preictal and interictal states on a per-subject basis, and ii) the improved ability of the eigen-wavelet multivariate $\hat{H}_m^M$ to assess such differences.

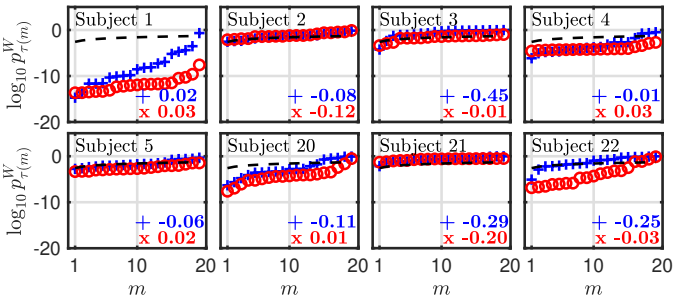

Fig. 4. **Preictal and interictal estimated selfsimilarity parameters distributions.** Sorted log p-values of the Wilcoxon signed-rank test between preictal and interictal estimated selfsimilarity parameters distributions for (blue '+') univariate $\hat{H}_m^U$ and (red 'o') eigen-wavelet multivariate $\hat{H}_m^M$ for the 8 different subjects, with the Benjamini-Hochberg (log-)thresholds (superimposed dashed black lines) at false discovery rate $\alpha = 0.05$. Corresponding significance scores averaged across components (cf. Eq. (6)) are reported at bottom right corner with corresponding colors and symbols.

D. Preictal state detection performance, per subject

To further quantify the benefits of multivariate selfsimilarity analysis to detect preictal states on a per-subject basis, receiver operating characteristic (ROC) curves are computed. For each subject independently, 100 interictal windows are first selected randomly, from which selfsimilarity exponents are estimated and used to define the empirical distributions of the $\hat{H}_m$ under the null hypothesis (interictal state). Second, for the same subject, for all available preictal windows and an equivalent number N_w of interictal windows chosen randomly (not from the set of the 100 windows used to create the distributions for the null hypothesis), selfsimilarity exponents are estimated. Third, from these estimates, p-values are computed by comparisons against the distributions of estimates $\hat{H}_m$ under null hypothesis and compared to Benjamini-Hochberg multiple comparison correction thresholds, for a collection of preset false discovery rates α. An interictal state rejection decision is taken as long as one of the $M = 19$ p-values is lower than the corresponding threshold. Fourth, averaging these decisions across the N_w preictal and interictal windows permit the computation of probabilities of correct detection and of false alarms for each preset false discovery rates α. These empirical probabilities are plotted one against the other to yield ROC curves.

This procedure is performed independently for the $M = 19$ univariate estimates $\hat{H}_m^U$, for the $M = 19$ eigen-wavelet multivariate estimates $\hat{H}_m^M$ and for the $M(M-1)/2 = 171$ classical multivariate estimates $\hat{H}_{m,m'}$. Fig. 5 compares, for each of the 8 subjects independently, the resulting ROC curves and related area under curve (AUC) for $\hat{H}_m^U$ (blue lines with '+'), for $\hat{H}_m^M$ (red lines with 'o') and for $\hat{H}_{m,m'}$ (black lines with 'Δ'). Fig. 5 shows that the eigen-wavelet multivariate

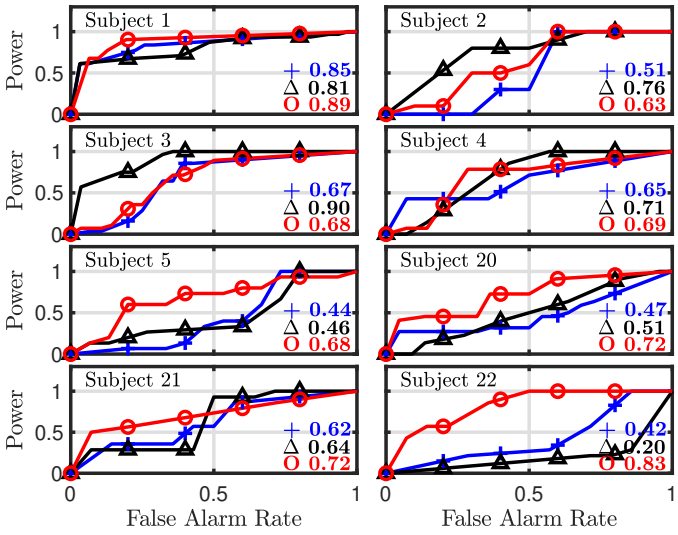

Fig. 5. **Epilepsy prediction from selfsimilarity exponent estimates.** ROC curves and related AUC of the test decisions for rejecting preictal states using (blue '+') univariate-like estimates $\hat{H}_m^U$, (black 'Δ') classical multivariate estimates $\hat{H}_{m,m'}$ and (red 'o') eigen-wavelet multivariate estimates $\hat{H}_m^M$ distributions for the different subjects.

approach reaches overall the most satisfactory performance: First, it always outperforms the univariate strategy; second, while it is outperformed by the classical multivariate strategy for one subject (Subject 2), it essentially does as well as and sometimes significantly better (Subjects 21 and 22) than the classical multivariate strategy – which may show poor sensitivity – while performing only $M = 19$ instead of $M(M-1)/2 = 171$ tests.

V. Conclusion and Perspectives

The present work has shown the relevance of comparing, on a per-subject basis, the scalefree temporal dynamics of multichannel scalp EEG data, in intericatal and preictal states for epilectic seizure prediction. It has also shown that multivariate scalefree temporal dynamics assessed by the eigen-wavelet multivariate selfsimilarity analysis described here outperforms univariate analysis or classical multivariate analyses. Indeed, the eigen-wavelet multivariate selfsimilarity analysis takes advantage of cross-temporal dynamics in EEG signals, which thus turns out to be useful for epilectic seizure prediction. Compared to classical multivariate analysis, the eigen-wavelet multivariate selfsimilarity analysis works even when mixing exist and relies on only M tests instead of $M(M-1)/2$. Finally, the proposed approach allows for the joint analysis of a large amount of channels, so that no channel selection step is needed before analysis. Matlab routines for multivariate selfsimilarity parameter estimation are publicly available at https://github.com/charlesglucas/ofbm_tools.

References

[1] B. J. He, "Scale-free properties of the functional magnetic resonance imaging signal during rest and task," *J. Neurosci.*, vol. 31, no. 39, pp. 13786–13795, 2011.

[2] P. Ciuciu, P. Abry, and B. J. He, "Interplay between functional connectivity and scale-free dynamics in intrinsic fMRI networks," *Neuroimage*, vol. 95, pp. 248–263, 2014.

[3] D. La Rocca, N. Zilber, P. Abry, V. van Wassenhove, and P. Ciuciu, "Self-similarity and multifractality in human brain activity: A wavelet-based analysis of scale-free brain dynamics," *J. Neurosci. Methods*, vol. 309, pp. 175–187, 2018.

[4] P. Abry and G. Didier, "Wavelet estimation for operator fractional Brownian motion," *Bernoulli*, vol. 24, no. 2, pp. 895–928, 2018.

[5] G. Didier and V. Pipiras, "Integral representations and properties of operator fractional Brownian motions," *Bernoulli*, vol. 17, no. 1, pp. 1–33, 2011.

[6] P. Abry and G. Didier, "Wavelet eigenvalue regression for n-variate operator fractional Brownian motion," *J. Multivar. Anal.*, vol. 168, pp. 75–104, November 2018.

[7] G. MohanBabu, S. Anupallavi, and S. R. Ashokkumar, "An optimized deep learning network model for eeg based seizure classification using synchronization and functional connectivity measures," *J. Ambient Intell. Humaniz. Comput.*, vol. 12, no. 7, pp. 7139–7151, 2021.

[8] F. Mormann, K. Lehnertz, P. David, and C. Elger, "Mean phase coherence as a measure for phase synchronization and its application to the eeg of epilepsy patients," *Phys. D: Nonlinear Phenom.*, vol. 144, no. 3-4, pp. 358–369, 2000.

[9] Y. Park, L. Luo, K. K. Parhi, and T. Netoff, "Seizure prediction with spectral power of eeg using cost-sensitive support vector machines," *Epilepsia*, vol. 52, no. 10, pp. 1761–1770, 2011.

[10] Z. Zhang and K. K. Parhi, "Low-complexity seizure prediction from ieeg/seeg using spectral power and ratios of spectral power," *IEEE Trans. Biomed. Circuits Syst.*, vol. 10, no. 3, pp. 693–706, 2015.

[11] D. EPMoghaddam, S. A. Sheth, Z. Haneef, J. Gavvala, and B. Aazhang, "Epileptic seizure prediction using spectral width of the covariance matrix," *J. Neural. Eng.*, vol. 19, no. 2, p. 026029, 2022.

[12] S. Janjarasjitt and K. A. Loparo, "Examination of scale-invariant characteristics of epileptic electroencephalograms using wavelet-based analysis," *Comput. Electr. Eng.*, vol. 40, no. 5, pp. 1766–1773, 2014.

[13] H. Daoud and M. A. Bayoumi, "Efficient epileptic seizure prediction based on deep learning," *IEEE Trans. Biomed. Circuits Syst.*, vol. 13, no. 5, pp. 804–813, 2019.

[14] S. Modak, S. S. Roy, R. Bose, and S. Chatterjee, "Focal epileptic area recognition employing cross eeg rhythm spectrum images and convolutional neural network," *IEEE Sens. J.*, vol. 21, no. 20, pp. 23335–23343, 2021.

[15] S. S. Roy, S. Modak, S. Roy, and S. Chatterjee, "Cross-wavelet transform aided focal and non-focal electroencephalography signal classification employing deep feature extraction," in *Modelling and Analysis of Active Biopotential Signals in Healthcare, Volume 2*, IOP Publishing, 2020.

[16] T. Alotaiby, F. E. A. El-Samie, S. A. Alshebeili, and I. Ahmad, "A review of channel selection algorithms for eeg signal processing," *Eurasip J. Adv. Signal Process.*, vol. 2015, pp. 1–21, 2015.

[17] K. Gadhoumi, J. Gotman, and J.-M. Lina, "Scale invariance properties of intracerebral eeg improve seizure prediction in mesial temporal lobe epilepsy," *PLoS one*, vol. 10, no. 4, p. e0121182, 2015.

[18] O. D. Domingues, P. Ciuciu, D. La Rocca, P. Abry, and H. Wendt, "Multifractal analysis for cumulant-based epileptic seizure detection in eeg time series," in *2019 IEEE 16th Int. J. Biomed. Imaging (ISBI 2019)*, pp. 143–146, IEEE, 2019.

[19] C.-G. Lucas, P. Abry, H. Wendt, and G. Didier, "Bootstrap for testing the equality of selfsimilarity exponents across multivariate time series," in *Proc. Eur. Signal Process. Conf. (EUSIPCO)*, (Dublin, IE), August 2021.

[20] A. L. Goldberger, L. A. Amaral, L. Glass, J. M. Hausdorff, P. C. Ivanov, R. G. Mark, J. E. Mietus, G. B. Moody, C. K. Peng, and H. E. Stanley, "Physiobank, physiotoolkit, and physionet: components of a new research resource for complex physiologic signals," *circulation*, vol. 101, no. 23, pp. e215–e220, 2000.

[21] V. Pipiras and M. S. Taqqu, *Long-Range Dependence and Self-Similarity*, vol. 45. Cambridge University Press, 2017.

[22] H. Wendt, G. Didier, S. Combrexelle, and P. Abry, "Multivariate Hadamard self-similarity: testing fractal connectivity," *Physica D*, vol. 356-357, pp. 1–36, 2017.

[23] S. Mallat, *A Wavelet Tour of Signal Processing*. San Diego, CA: Academic Press, 1998.

[24] Y. Benjamini and Y. Hochberg, "Controlling the false discovery rate: a practical and powerful approach to multiple testing," *J. R. Stat. Soc., B: Stat. Methodol.*, vol. 57, no. 1, pp. 289–300, 1995.